



Semnan University

Mechanics of Advanced Composite Structures

journal homepage: <http://MACS.journals.semnan.ac.ir>

Distribution of Residual Stresses in Polymer Reinforced Carbon Nanotubes and Laminated Carbon Fibers

A.R. Ghasemi*, M. Mohammadi-Fesharaki

Department of Solid Mechanics, Faculty of Mechanical Engineering, University of Kashan, Kashan, Iran

PAPER INFO

Paper history:

Received 2016-07-23

Revised 2016-09-23

Accepted 2016-10-02

Keywords:

Residual stresses

Carbon nanotube

Nanocomposite

Unit cell

ABSTRACT

In this study, the distribution of residual stress in fiber-reinforced nanocomposites is investigated. Fiber-reinforced nanocomposite is composed of three substances: carbon fiber, carbon nanotube (CNT), and polymer matrix. Unit cells in hexagonal packing array with different arrays as unit cell, 3*3 and 5*5 arrays have been selected as suitable for finite element analysis of residual stresses. Radial and tangential residual stress have been determined in different directions by finite element analysis using ABAQUS commercial software for each phase individually. The effect of the CNTs' various volume fractions (0%, 1%, 2%, and 3%) on residual stress distribution has been studied in different directions and compared to one another for each phase. Results show that the 3*3 unit cells arrays are suitable for modeling micro-residual stresses, and the results of this array are reliable. In addition, adding a 3% volume fraction of CNTs to the matrix is the best option for reduction of overall residual stresses with minimal fluctuation in local micro-residual stresses.

DOI: 10.22075/MACS.2016.476

© 2017 Published by Semnan University Press. All rights reserved.

1. Introduction

Because of many favorable properties of composite materials high stiffness, strength, and corrosion resistance, to name a few-these materials quickly found a special position in the industry. The high strength-to-weight ratio of polymer matrix composites (PMCs) has caused this type of composite substance to be often-used. Curing is a production step in the manufacture of PMC components, and the distinct coefficient thermal expansion (CTE) properties of various constituent components can cause residual thermal stresses to be created in the cooling step.

The distribution of residual stresses is characterized as macro- or micro-residual stress. Macro-residual stresses are caused by interlaminar deformations in composite laminate layers, caused to varying CTE directional properties of the layers. Micro-residual stresses develop due to varying CTEs within the constituent phases. In the field of micro-residual stress distribution, Hann and Pagona [1] formulated a

method based on total stress-strain-temperature relations to determine the curing stresses in boron/epoxy composite and found the method to be preferable to the incremental method. More recently, Shokrieh and Ghasemi [2-3] presented a new method for calculating calibration factors for measuring residual stresses in composite laminate materials. Calibration factors of incremental hole-drilling correlated the released strains to the residual stresses in each layer. Because of the non-uniform distribution of residual stresses through the thickness of each specimen, the integral method was used for determination of residual stresses in laminated composites.

Ghasemi et al. [4] employed the integral hole drilling method to calculate the non-uniform residual stresses in various composite laminates. Three ply configurations-symmetric cross-ply, asymmetric cross-ply and symmetric quasi-isotropic specimens-used to study the model's ability to predict residual stresses; the model produced results that agreed with theoretical results. Ghasemi and Mohammadi

*Corresponding author. Tel.: +98-31-55912426; Fax: +98-31-55912424

E-mail address: ghasemi@kashanu.ac.ir

[5-6] used integral method for the approximation of residual stresses field in fiber-metal laminates (FMLs). They experimented with an incremental hole-drilling method to measure the non-uniform residual stresses in each FML ply. The results showed close agreement with predictions using classical laminate plate theory.

Abouhamzeh et al. [7] presented an analytical model to predict warpage and residual stresses that develop during FML curing. They implemented change of stiffness and chemical shrinkage of the material during curing in the model. In the field of micro-residual stresses, common methods for determining residual stresses include finite element analysis [8-12], circular disc model (CDM) [13-14], cylinder theory [15-17], and energy method [18-20]. Levin et al. [21] studied residual stresses in an Alumina-SiC particulate composite as a function of silicon carbide (SiC) content by X-ray diffraction. According to X-ray reflection shift and line broadening analysis, average micro-residual stresses evaluated in each phase. Todd et al. [22] repeated measuring of micro-residual stresses in Alumina-SiC by neutron diffraction. Wu [23] used an analytical charge distortion model (CDM) for measuring micro-residual stresses in Alumina-SiC nanocomposite and compared his results with the experimental results presented by Levin et al. The comparison showed good agreement and certified CDM results. Maligno [24] investigated the effect of micro-residual stresses on damage of fiber-reinforced laminates as finite element modeling of a unit cell. Residual stresses introduced by curing were determined by considering two possibilities: 1) volume shrinkage of the matrix resin from the crosslink polymerization during isothermal curing and, 2) thermal contraction of both resin and fiber as a consequence of the cooling process to room temperature.

Moreno and Marques [25] considered a different configuration of unit cells and boundary conditions to identify effective properties of active fiber composites (AFCs). AFCs are composed of uniaxial-oriented piezoceramic fibers embedded in a polymer matrix that is sandwiched between two interdigitated electrodes that can be designed as sensors and actuators for applications such as structure-health monitoring and vibration control. They compared results to past researches and showed good agreement. Shokrieh and Ghanei-Mohammadi [26] investigated finite element analysis of residual stresses in fiber-reinforced laminate composites. Three types of representative volume element configurations-circular, square and hexagonal modeled were tested, and the effect of each type of fiber packing was studied. They examined the effect of fiber neighbor and boundary conditions on the residual stress distribution of different unit cells and introduced new boundary conditions

for the monofiber model to enable it to predict macro-behavior in an efficient way. Shokrieh and Sa-farabadi [27] used the energy method to identify micro-residual stresses in cylinder unit cells. They considered the interphase region between the fiber phase and the matrix phase, as well as the effect of interphase thickness on axial, radial, and shear residual stresses in unit cells.

In three-phase composite materials, Shokrieh et al. [28] used carbon nanotubes (CNTs) in fiber-reinforced laminate composites. Using polymer matrix, they investigated the effect of CNTs on the reduction of residual stresses by the energy method and slitting method. Another nanomaterial that is used to reduce residual stresses is carbon nanofiber. Ghasemi et al. [29] studied the effect of carbon nanofibers (CNFs) on the reduction of thermal residual stresses in fiber-reinforced composite materials. Micromechanical models are used for determining mechanical and thermal properties of three-phase composites, including carbon fiber, CNT, and polymer matrix. Ghasemi and Mohammadi [30-32] studied the distribution of residual stresses in three-phase composite materials used in CNTs as reinforcement of carbon fiber by the electrophoresis method in laminate composites. They used CDM, cylinder theory, and finite element analysis to determine residual stresses in every phase individually.

In this paper, distribution of residual stresses is investigated in the three phases of fiber-reinforced nanocomposite, including carbon fiber, CNT, and polymer matrix. Residual stress distribution is studied in different unit-cell arrays to select an ideal array for this analysis. Radial and tangential residual stress is studied in every phase separately, and the effect of 0%, 1%, 2% and 3% CNT volume fractions on residual stresses is studied in different directions.

2. Unit Cell

Representative volume element (RVE), or unit cell, is a qualified representation element for micro-mechanical analysis of fiber-reinforced, unidirectional laminate composites. For unit cells, the ideal regular arrangement of reinforcing fibers is assumed to be in the matrix. Square-packing array and hexagonal-packing array are two prevalent arrays used for unidirectional fiber-reinforced composite laminates. Schematics of these arrays are shown in Fig. 1. Hexagonal packing array is more useful and suitable for residual stress analysis than is square-packing array [24]; hence; it is the focus of this paper.

Because of the high mechanical and thermal properties of nanomaterials, they are used as additional substances in composite materials. Nanomaterials improve mechanical and thermal properties of composite materials. CNTs are typically dispersed into

the polymer matrix to reinforce composite materials. The reinforced matrix is, in turn, used as a new matrix for unidirectional fibers. Mechanical and thermal properties of carbon fiber, epoxy matrix, and CNT are shown in Table 1. E , α_T , and ν are elastic modulus, transverse CTE, and Poisson's ratio, respectively.

CNTs should be homogeneously distributed in the matrix to improve the mechanical properties of nanocomposites. Unit cells with homogenous dispersion of 1% CNT volume fraction and 60% carbon-fiber volume fraction are shown in Fig. 2(a).

The CNT and carbon fiber radii are considered equal ($4 \text{ e-}5 \text{ mm}$ and $3.25 \text{ e-}3 \text{ mm}$) and corresponding to actual dimensions. Three different directions are selected to determine residual stress distribution: 1) around the central carbon fiber, 2) OP direction, and 3) OQ direction, as shown in Fig. 2(b). Boundary conditions of residual stresses analysis for unit cells are shown in Fig. 2(b). According to Zhao et al. [33], these are qualified boundary conditions for residual stress analysis.

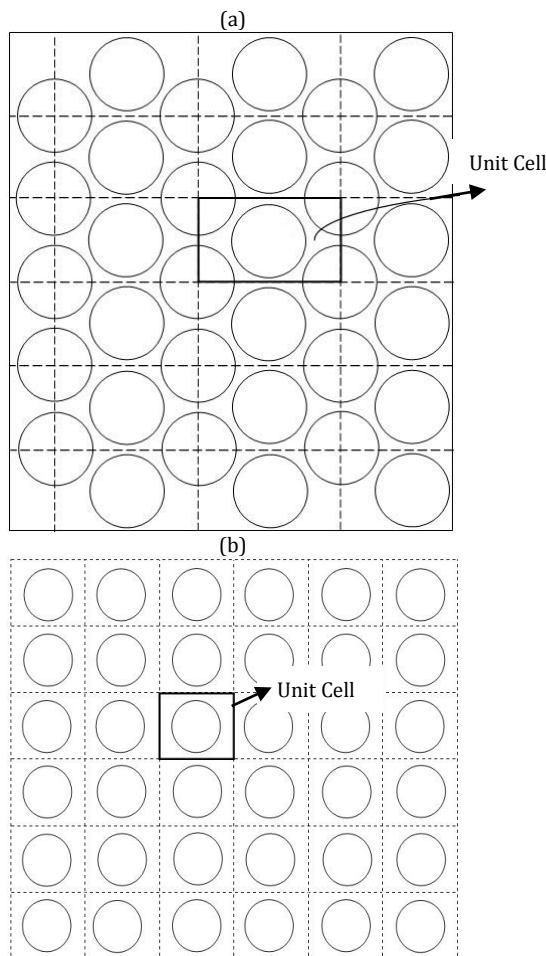


Figure 1. Schematic of unit cell; (a) hexagonal packing array and (b) square packing array.

Table 1. Mechanical and thermal properties of various phases [30].

Phase	E (GPa)	α_T ($1/^\circ\text{C}$)	ν
Carbon fiber	230	15 e-6	0.2
CNT	1000	15 e-6	0.1
Epoxy ML506	3.13	62.45e-6	0.35

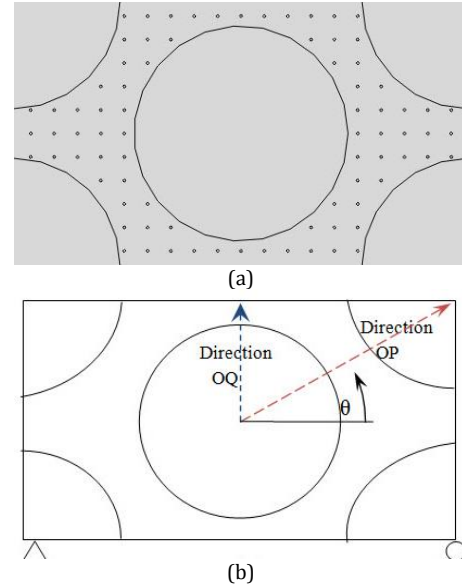


Figure 2. Unit cell schematics: (a) homogenous dispersion of CNTs and (b) boundary conditions and different directions.

3. Finite Element Modeling

ABAQUS commercial software was used for finite element modeling and residual stress analysis in different arrays and different CNT volume fractions. Unit cells were modeled as two dimensional and simply supported boundary conditions are applied around the plate, as shown in Fig. 2(b). Curing temperature was considered equal to $120 \text{ }^\circ\text{C}$, and $\Delta t = 100 \text{ }^\circ\text{C}$ was considered for residual stress analysis with respect to an ambient temperature of $20 \text{ }^\circ\text{C}$. The cooling process, from curing temperature to ambient temperature, is applied smoothly and neglected changes of mechanical and thermal properties of every phase. For example, the finite element modeling of a unit cell, 3×3 and 5×5 arrays of 1% CNT volume fraction are shown in Figs. 3(a), 3(c), and 3(d) as two dimensional, respectively. A part of a unit cell composed of three phases is shown in Fig. 3(b) in very fine detail. The CNTs are modeled according to actual dimensions, and mechanical and thermal properties. Considered as a triangle, CPS4R is the carbon fiber and CNT's element type, and CPS3 is the matrix element type. The approximate global size is equal to $18 \text{ e-}5 \text{ (mm)}$; the 3×3 unit-cell array model comprises 22,442 elements, and the 5×5 array models comprise 201,978 and 561,050 elements, respectively.

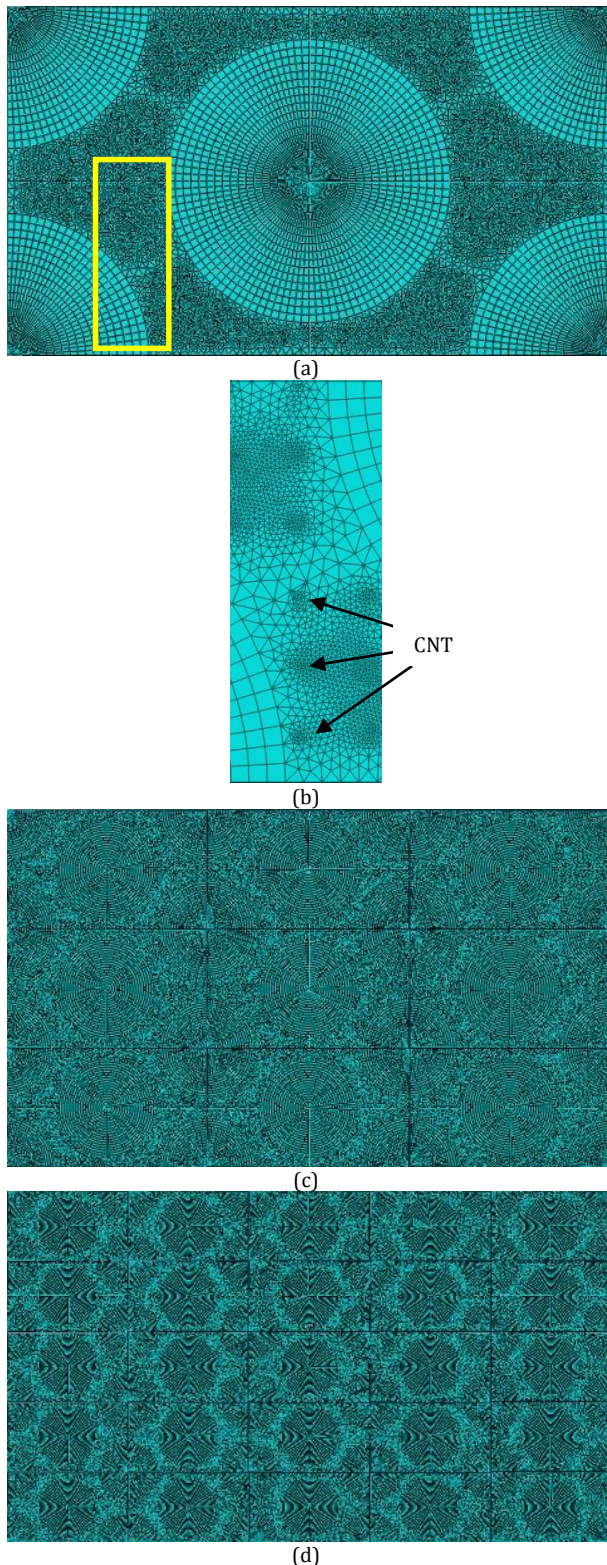


Figure 3. Unit cell Finite element modeling: (a) unit cell, (b) zone of unit cell elements, (c) 3*3 array and (d) 5*5 array.

4. Comparison of Arrays

In order to consider the neighborhood conditions of carbon fiber and more adaptability of modeling to

actually, two other additional arrays were considered for comparing residual stress distribution and selection of suitable arrays for analysis. To study the residual stresses in different arrays, the unit cell was considered two-phased, with 60% carbon fiber volume fraction and without CNT.

The distribution of radial residual stress for different unit cell arrays around the central carbon fiber is shown in Fig. 4. In all cases, radial residual stress distribution is symmetric around the central carbon fiber and is consistent with real conditions. The distribution of radial residual stress around the central carbon fiber in various arrays indicates that increasing the number of carbon fibers caused converged radial residual stress distribution results. The stress distribution in the 3*3 and 5*5 arrays around the central carbon fiber were close together and functioned differently than they would separately in a unit cell. Neighborhood conditions caused the carbon fiber to change locations, affecting the magnitude of the maximum residual stress around central carbon fiber in both arrays. The maximum radial residual stress distribution difference between the 3*3 and 5*5 arrays is less than 7%; however, the radial residual stress distribution of a unit cell is completely different than that of other arrays. This shows that the effect of neighboring carbon fibers is not negligible.

The tangential residual stress distribution around the central carbon fiber is shown in Fig. 5. Change of residual stresses around it is due to the effect of neighboring carbon fibers. Distribution of tangential residual stress converges by increasing the amount of carbon fiber, as the maximum difference of tangential residual stresses in 3*3 and 5*5 arrays is less than 2%. For the unit cell array, the magnitude and the distribution of tangential residual stresses are so different with other arrays, as 3*3 array and 5*5 array, that shows no accuracy of the unit cell array.

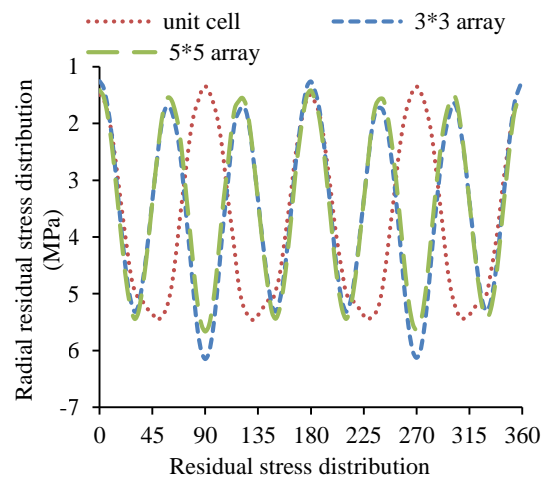


Figure 4. Radial residual stress distribution around the central carbon fiber for different arrays.

The OP direction is considered the direction between two carbon fibers. Radial residual stress distribution is investigated in the OP direction for different arrays in Fig. 6. For a unit cell, radial residual stress distribution is zero at the end of the OP direction. In this location, radial residual stresses did not equal zero for 3*3 and 5*5 arrays due to existence and increase of neighboring carbon fibers.

For the 3*3 and 5*5 arrays, the radial residual stress distribution is very close together, as the maximum radial residual stress difference in the arrays is less than 8%. Radial residual stress distribution is symmetric in the OP direction from the central carbon fiber to the neighboring carbon fiber; however, due to free stress at the edge in the unit cell array, the radial residual stress distribution was not symmetric in the OP direction.

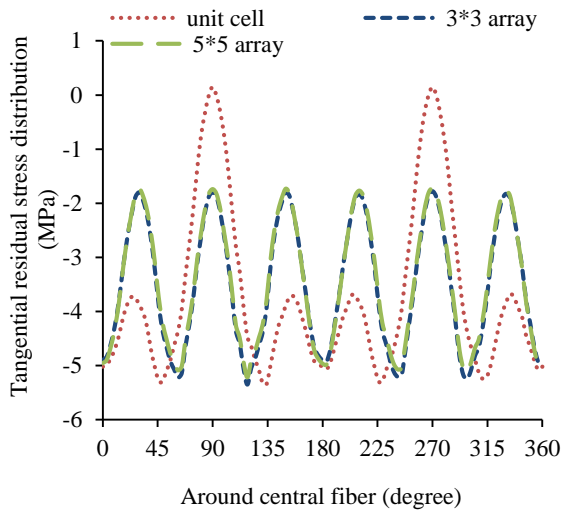


Figure 5. Tangential residual stress distribution around central fiber for different arrays.

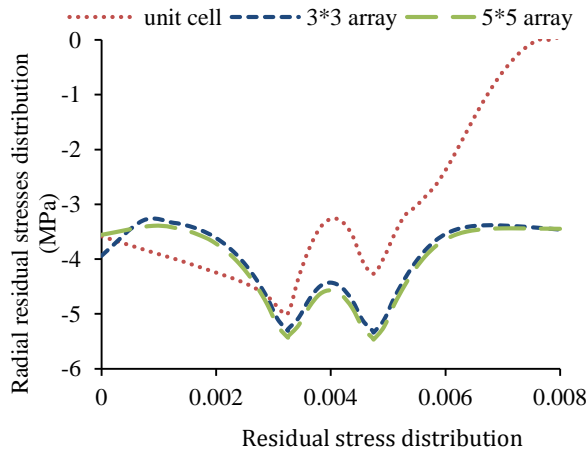


Figure 6. Radial residual stress distribution in the OP direction for different arrays.

The tangential residual stress distribution of different arrays in the OP direction is shown in Fig. 7. Tangential residual stresses are compressive in carbon fiber and tensional in resin matrix. In unit cells, tangential residual stress distribution is asymmetrical, but increasing the number of carbon fibers caused symmetric distribution of tangential residual stresses in the 3*3 and 5*5 arrays. Tangential residual stress distribution converged when the number of carbon fibers increased, so tangential residual stress distribution was very close together in both arrays.

Radial residual stress in the OQ direction is shown in Fig. 8. In the unit cell, radial residual stresses were decreased in the carbon fiber and matrix from -3.57 (MPa) in the central fiber to the OQ's free stress edge. Increasing the number of carbon fibers caused a change in the radial residual stress distribution in both arrays as a result of neighboring carbon fibers. Radial residual stresses are increased to the carbon fiber and matrix boundaries in both arrays, where radial residual stresses are decreased from the edge of the central carbon fiber to the end of OQ direction. Radial residual stress distribution of the 3*3 and 5*5 arrays are close together and the maximum difference of radial residual stress in the 3*3 and 5*5 arrays became less than 9%. Tangential residual stress distribution for different arrays in the OQ direction is shown in Fig. 9. Tangential residual stresses become compressive in carbon fiber and tensional in the resin matrix. Increasing number of carbon fibers caused tangential residual stress results to converge in this direction, as well; somehow the 3*3 and 5*5 arrays coincided in every phase.

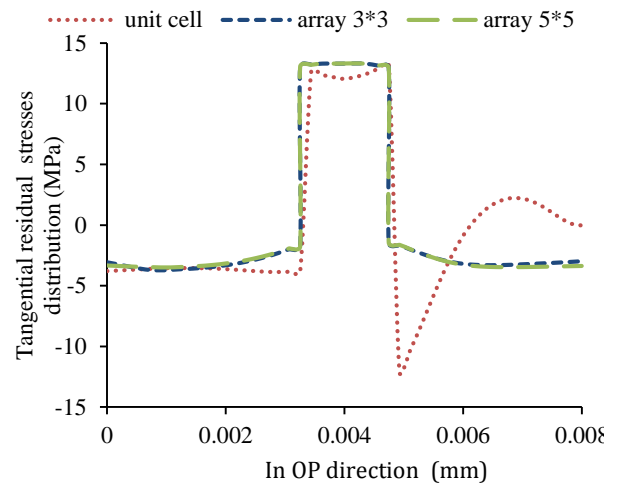


Figure 7. Tangential residual stress distribution in the OP direction for different arrays.

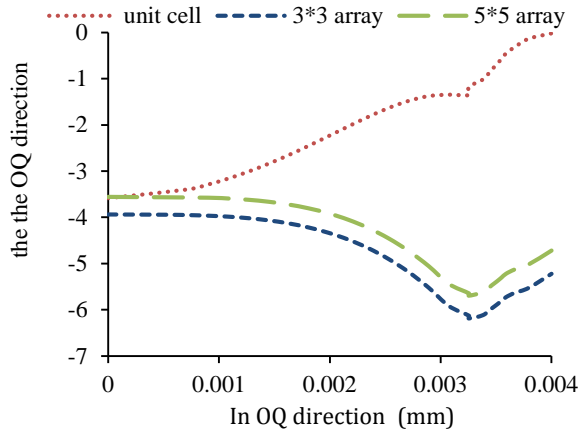


Figure 8. Radial residual stress distribution in the OQ direction for different arrays.

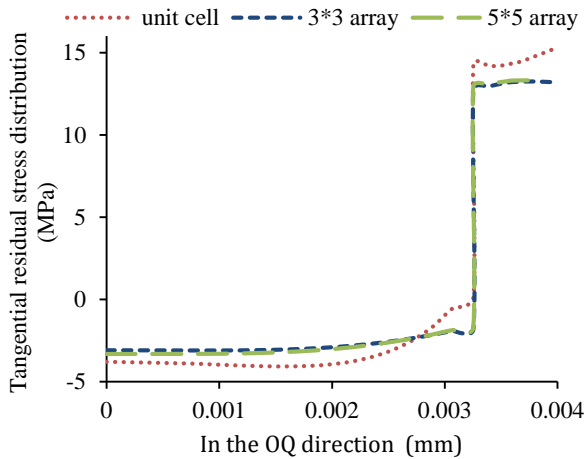


Figure 9. Tangential residual stress distribution in the OQ direction for different arrays.

According to the radial and tangential residual stress distribution in different arrays for the two-phase unit cell (60% carbon fiber and 0% CNT volume fraction), the increasing number of carbon fibers caused the results to converge and be more logical. The distribution of residual stresses in 3*3 array are so close to 5*5 array that shows stable results and considering more array do not have significant effect on the residual stress distribution. In this research, 3*3 array is selected between different arrays due to better results respect to the unit cell array and less time for the finite element analysis respect to 5*5 array.

5. The effect of adding CNTs on residual stress distribution

Four different CNT volume fractions (0%, 1%, 2%, and 3%) with a constant 60% volume fraction of carbon fiber were employed to evaluate the effect of additional CNTs on residual stress distribution. Dispersion of CNTs in the matrix must be homogenous to have a sufficient effect on it.

Schematic modeling of homogenous dispersion of different CNT volume fractions is shown in Fig. 10. According to homogenous CNT dispersion, and considering actual CNT size, increasing the CNT volume fraction changed the number of CNTs in select directions and in the distance between one another. A CNT stayed in the OP direction certainly for the 2% CNT volume fraction only. As shown in Fig. 10, the number of CNTs in the OP and OQ directions is different in various cases.

In this section, radial and tangential residual stress distribution is investigated in different directions for different CNT volume fractions. The comparison of residual stress distribution of different arrays in the previous section show that the 3*3 array is suitable for determining residual stress distribution in a different direction. Radial residual stress distribution around the central carbon fiber for different CNT volume fractions is shown in Fig. 11.

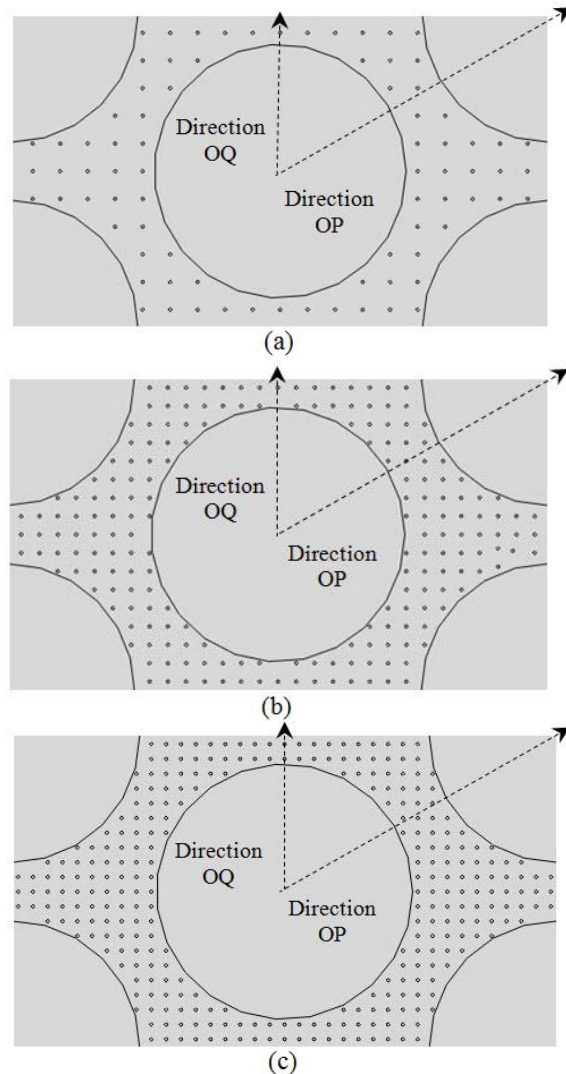


Figure 10. Unit cell with different CNT volume fractions: a) 1% CNT; b) 2% CNT; c) 3% CNT.

Maximum and minimum radial residual stress distribution occurred where adjacent carbon fibers were at a maximum and minimum distance from the central carbon fiber in the 0% CNT volume fraction. The existence of CNTs caused a change in the location and magnitude of radial residual stress. Increasing and neighborhood of CNT to carbon fiber caused a fluctuation in radial residual stress.

Tangential residual stress distribution around the central carbon fiber is shown in Fig. 12. Adding CNTs caused the magnitude and location of maximum and minimum tangential residual stress distribution to change. For the 0% CNT volume fraction, tangential residual stress distribution is smoother than other cases because of the CNTs effect on tangential residual stress distribution. For the 1%, 2%, and 3% CNT volume fractions, adding CNTs caused a fluctuation of tangential residual stress in the central carbon fiber.

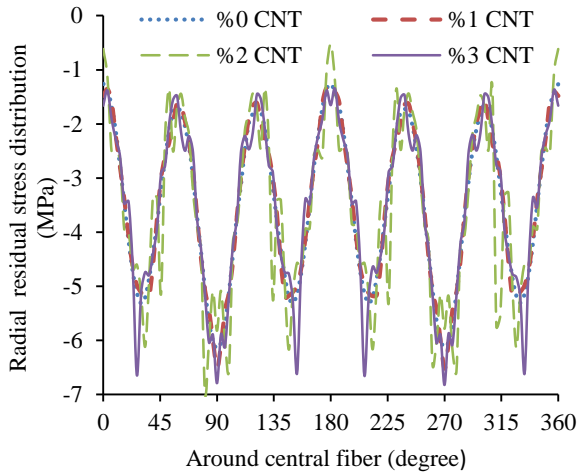


Figure 11. Radial residual stress distribution around fiber for different CNT volume fractions.

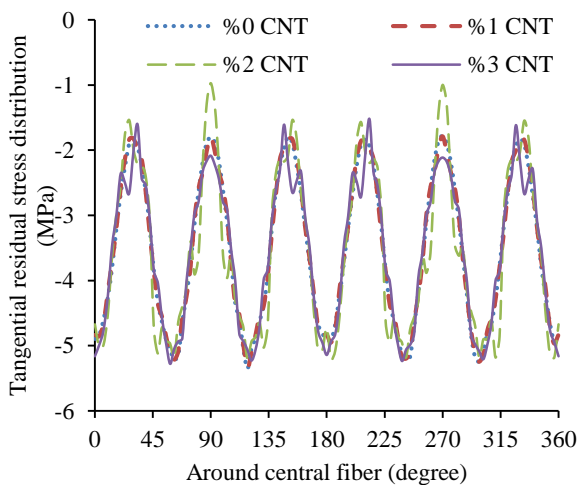


Figure 12. Tangential residual stresses distribution around fiber for different CNT volume fractions.

The radial residual stress distribution in the OP direction is shown in Fig. 13. The distribution became symmetric, so the magnitude of radial residual stress in the central fiber carbon and neighboring carbon fiber is similar in the OP direction. The presence of CNTs, along with their increase, caused non-uniformity of the radial residual stress distribution in the matrix. However, no significant change in residual stress distribution occurred in the carbon fibers. For the 2% CNT volume fraction, the radial residual stress increased suddenly from -5.14 (MPa) in the matrix to -24.8 (MPa) in the CNTs. This sudden change is due certainly to the presence of CNTs in the OP direction. In the case of the 3% CNT volume fraction, a greater number of CNTs are present near the OP direction. The effect of these CNTs was fluctuation of the radial residual stress distribution in the matrix.

Fluctuation of the radial residual stress distribution is the reason for the increasing CNTs adjacent to the OP direction for the 1% and 3% CNT volume fraction, but the sudden change in radial residual stress distribution for the 2% CNT volume fraction accounts for the existence of a CNT in this direction (Fig. 10(b)).

Tangential residual stress distribution in the OP direction is shown in Fig. 14. Tangential residual stresses become compressive residual stresses in carbon fiber and tensile residual stresses in the matrix. The existence of CNTs is caused by the non-uniformity of the tangential residual stress in the matrix. Tangential residual stress distribution is symmetric for the 0% and 1% CNT volume fractions. Regarding the 2% CNT volume fraction, the existence of a CNT in the OP direction changed the tangential residual stress from 13.4 (MPa) in the matrix to 9.2 (MPa) in the CNT, so the tangential residual stress equaling 9.2 (MPa) is the magnitude of the tangential residual stress in the CNT in this case. For the 3% CNT volume fraction, the effect of the CNTs near the OP direction in the matrix caused fluctuation of the tangential residual stress.

Radial residual stress distribution in the OQ direction is shown in Fig. 15. For the 0% CNT volume fraction, the distribution of radial residual stresses was uniform. By adding CNT to the matrix, some CNTs placed on OQ direction that caused to change the distribution of radial residual stresses. For the 1% CNT volume fraction, radial residual stresses changed from -5.76 (MPa) in the matrix to -25.5 (MPa) in CNT. Regarding the 2% CNT volume fraction, as CNT location changed, the position of the radial residual stress peak changed to CNT location. And for the 3% CNT volume fraction, two CNTs in the OQ direction caused radial residual stresses to change from 6.82 (MPa) in the matrix to -26.17 (MPa) in CNT. This change of radial residual stress occurred for the second CNT in the OQ direction from -7.95 (MPa) in the matrix to -23.7 (MPa) in CNT.

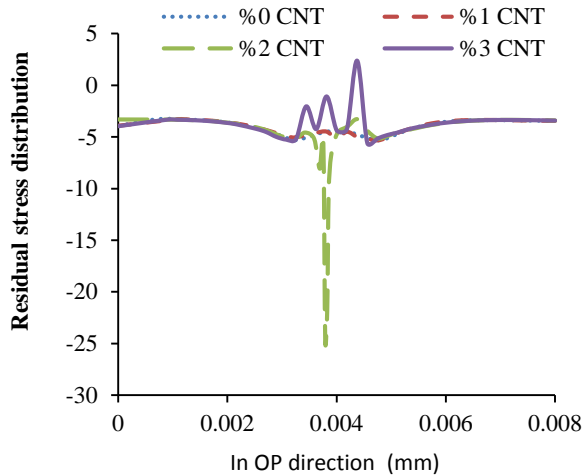


Figure 13. Radial residual stress distribution in the OP direction for different CNT volume fractions.

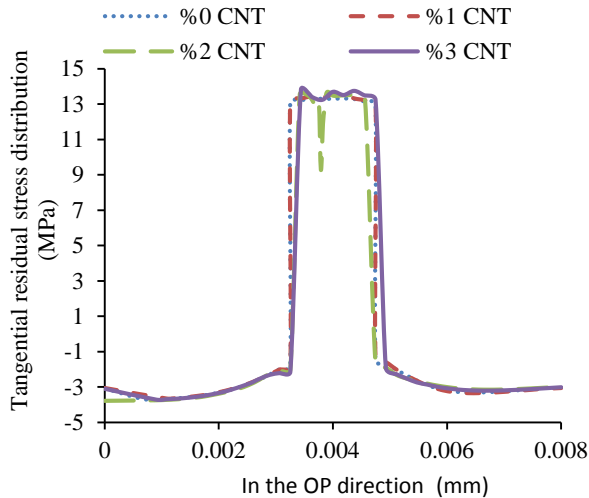


Figure 14. Tangential residual stress distribution in the OP direction for different CNT volume fractions.

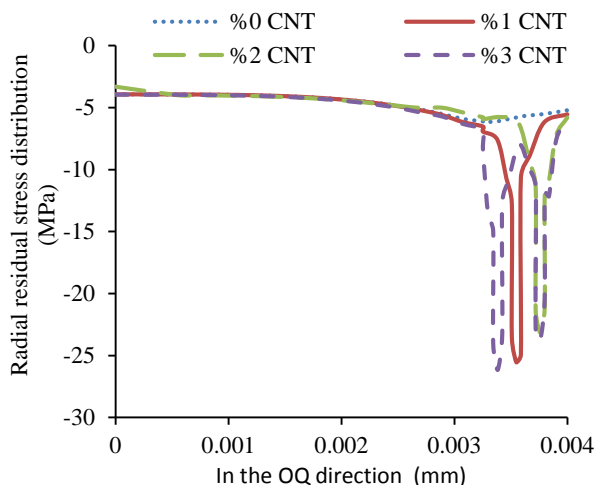


Figure 15. Radial residual stress distribution in the OQ direction for different CNT volume fractions.

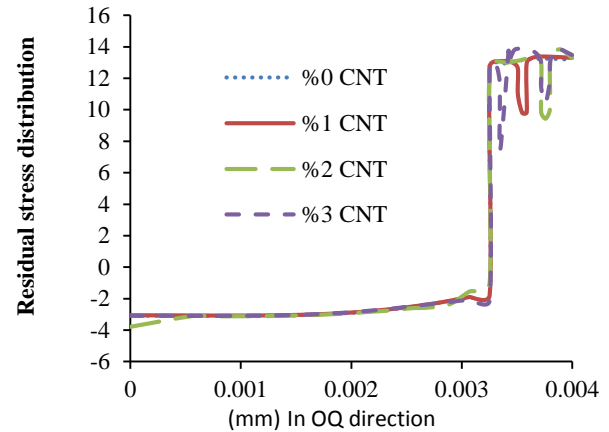


Figure 16. Tangential residual stress distribution in the OQ direction for different CNT volume fractions.

Table 2. Tangential residual stresses in the OQ direction (MPa).

%CNT	Fiber Phase	CNT Phase	Matrix Phase
%0	-3.09	-	13.25
%1	-3.08	9.79	13.37
%2	-3.08	9.40	13.40
%3	-3.10	10.47*	13.70
		7.36**	

* First CNT

** Second CNT

The distribution of tangential residual stresses in the OQ direction is displayed in Fig. 16. Tangential residual stresses became compressive in the carbon fiber and tensional in the CNT and matrix. Distribution of tangential residual stress became smooth in the absence of CNT. For the 1% CNT volume fraction, the presence of a CNT caused the tangential residual stresses to decrease from 13.37 (MPa) in the matrix to 9.79 (MPa) in the CNT. In the case of the 2% CNT volume fraction, the CNT location changed with respect to the 1% CNT volume fraction, causing the tangential residual stress peak to change locations. For the 3% CNT volume fraction case, two CNTs stayed in the OQ direction in the matrix, which caused the tangential residual stress to change suddenly, from 12.71 (MPa) in the matrix to 7.36 (MPa) in first CNT, and from 13.7 (MPa) in the matrix to 10.47 (MPa) in the second CNT. The magnitude of tangential residual stress for different cases in every phase are shown in Table 2.

6. Conclusions

The distribution of residual stresses for three-phase CNT/matrix/fiber composites has been investigated. ABAQUS commercial finite element software was used and residual stress in different directions of a unit cell were studied. The results showed that:

- The 3*3 arrays of a unit cell are suitable for modeling micro-residual stresses, and the results of this array are reliable.

- The magnitude and change of the distribution of tangential and radial residual stress are important and significant in different directions.
- Although adding the CNTs caused the fluctuation of tangential and radial residual stress, a decrease in residual stress occurred in composite materials.
- Although the presence of CNTs reduces overall residual stress in composite materials, the local residual stress in CNT particles is considerable.
- Adding a 3% volume fraction of CNTs to the matrix is the best option in these cases for reducing overall residual stress and maintaining minimum fluctuation in local micro-residual stress.

References

- [1] Hahn HT, Pagano NJ. Curing stresses in composite laminates. *J Compos Mater* 1975; 9(1): 91-106.
- [2] Shokrieh MM, Ghasemi AR. Simulation of central hole drilling process for measurement of residual Stresses in isotropic, orthotropic, and laminated composite plates *J Compos Mater* 2007; 41(4): 435-452.
- [3] Ghasemi AR, Shokrieh MM. Development of an integral method for determination of non-uniform residual stresses in laminated composites. *Iran J Polym Sci & Tech* 2008; 21(4): 347-355.
- [4] Ghasemi A, Taheri-Behrooz F, Shokrieh M. Determination of non-uniform residual stresses in laminated composites using integral hole drilling method: Experimental evaluation. *J Compos Mater* 2014; 48(4): 415-425.
- [5] Ghasemi AR, Mohammadi M. Calculation of calibration factors for determination of residual stresses in fiber-metal laminates using incremental hole-drilling method. *J Sci Tech Compos* 2014; 1(1): 35-44.
- [6] Ghasemi AR, Mohammadi M. Residual stress measurement of fiber metal laminates using incremental hole-drilling technique in consideration of the integral method. *Int J Mech Sci* 2016; 114: 246-256.
- [7] Abouhamzeh M, Sinke J, Jansen KMB, Benedictus R. Closed form expression for residual stresses and warpage during cure of composite laminates. *Compos Struct* 2015; 133: 902-910.
- [8] Chen Y, Xia Z, Ellyin F. Evolution of Residual Stresses Induced During Curing Processing Using a Viscoelastic Micromechanical Model. *Compos. Mater* 2001; 35: 522-542.
- [9] Aghdam MM, Khojeh A. More on the Effects of Thermal Residual and Hydrostatic Stresses on Yielding Behavior of Unidirectional Composites. *Compos Struct* 2003; 62: 285-290.
- [10] Karami G, Garnich M. Micromechanical Study of Thermoelastic Behavior of Composites with Periodic Fiber Waviness, *Compos Part B* 2005; 36: 241-248.
- [11] Zhao LG, Warrior N.A, Long AC. A Thermo-Viscoelastic Analysis of Process-Induced Residual Stress in Fibre-Reinforced Polymer-Matrix Composites, *Mater Sci Eng* 2007; 45: 483-498.
- [12] Jin KK, Huang Y, Lee Y, Sung KH. Distribution of MicroStresses and Interfacial Tensions in Unidirectional Composites. *Compos Mater* 2008; 42: 1825-1849.
- [13] Quek M. Analysis of Residual Stresses in a Single Fibre-Matrix Composite. *Int J Adhes Adhes* 2004; 24(5): 379-388.
- [14] Hsueh C H, Becher PF, Sun EY. Analyses of thermal expansion behavior of intergranular two-phase composites. *J Mater Sci* 2001; 36: 255-261.
- [15] Jayaraman K, Reifsnider KL. Residual Stresses in a Composite with Continuously Varying Young's Modulus in the Fiber/Matrix Interphase. *Compos Mater* 1992; 26: 770-791.
- [16] Jayaraman K, Reifsnider KL. The Interphase in Unidirectional Fiber-Reinforced Epoxies: Effect of Residual Thermal Stresses. *Compos Sci Technol* 1993; 47: 119-129.
- [17] Bianchi V, Goursat P, Menessier E. Carbon-Fiber-Reinforced YMAS Glass Ceramic Matrix - IV Thermal Residual Stresses and Fiber/Matrix Interfaces. *Compos Sci Technol* 1998; 58: 409-418.
- [18] Quek MY, Yue CY. Axisymmetric Stress Distribution in the Single Filament Pull out Test. *Mater Sci Eng* 1994; 189: 105-116.
- [19] Zhang Y, Xia Z, Ellyin F. Evolution and Influence of Residual Stresses/Strains of Fiber Reinforced Laminates. *Compos Sci Technol* 2004; 64: 1613-1625.
- [20] Song DY, Takeda N, Ogihara S. A Method of Stress Analysis for Interfacial Property Evaluation in Thermoplastic Composites. *Mater Sci Eng* 2000; 278: 242-246.
- [21] Levin I, Kaplan WD, Brandon D, Wieder T. Residual stresses in alumina-SiC nanocomposites. *Acta Metall Mater* 1994; 42(4): 1147-1154.
- [22] Todd R, Bourke M, Borsa C, Brook R. Neutron diffraction measurements of residual stresses in alumina/SiC nanocomposites. *Acta Mater* 1997; 45(4): 1791-1800.

- [23] Wu H. **Residual stresses in composite materials**. Woodhead Publishing; 2014.
- [24] Maligno AR. **Finite element investigations on the microstructure of composite materials**. Ph.D. Thesis, University of Nottingham, 2008.
- [25] Moreno MM, Marques FD. Influence of Boundary Conditions on the Determination of Effective Material Properties for Active Fiber Composites. *11th Pan-American Cong Appl Mech*; 2010.
- [26] Shokrieh MM, Ghanei-Mohammadi AR. Finite Element Modeling of Residual Thermal Stresses in Fiber-Reinforced Composites Using Different Representative Volume Elements. *World Cong Eng*; 2010.
- [27] Shokrieh MM, Safarabadi M. Three-dimensional analysis of micro residual stresses in fibrous composites based on the energy method: a study including interphase effects. *J Com Mat* 2012; 46(6): 727-735.
- [28] Shokrieh M, Daneshvar A and Akbari S. Reduction of thermal residual stresses of laminated polymer composites by addition of carbon nanotubes. *Mater Des* 2014; 53: 209-216.
- [29] Ghasemi AR, Mohammadi MM, Mohandes M. The role of carbon nanofibers on thermo-mechanical properties of polymer matrix composites and their effect on reduction of residual stresses. *Compos Part B* 2015; 77: 519-527.
- [30] Ghasemi AR and Mohammadi M. Three-dimensional residual stresses analysis of nanocomposite polymeric matrix based on fiber reinforced carbon nanotubes. *J Sci Tech Comp* 2016; 4(2): 23-30.
- [31] Ghasemi AR, Mohammadi M. Development of Circular Disk Model for Polymeric Nanocomposites and Micromechanical Analysis of Residual Stresses in Reinforced Fibers with Carbon Nanotubes. *Comput Methods Appl Mech Eng* 2017; 35(2): 177-196.
- [32] Ghasemi AR, Mohammadi-Fesharaki M, Mohandes M. Three-Phase Micromechanical Analysis of Residual Stresses in Reinforced Fiber by Carbon Nanotubes. *J Compos Mat* 2016; DOI: 10.1177/0021998316669854.
- [33] Zhao LG, Warrior LA, Long AC. A Micromechanical Study of Residual Stress and Its Effect on Transverse Failure in Polymer-Matrix Composites. *Int J sol struct* 2006; 43: 5449-5467.